A conceptual model-based sediment connectivity assessment for patchy agricultural catchments

Pedro V. G. Batista[1*], Peter Fiener[2], Simon Scheper[1, 3], Christine Alewell[1]

[1]Department of Environmental Sciences, Universität Basel, Bernoullistrasse 30, 4056, Basel, Switzerland.

[2]Institute for Geography, Universität Augsburg, Alter Postweg 118, 86159, Augsburg, Germany.

[3]Dr. Simon Scheper – Research | Consulting | Teaching, Eickhorst 3, 29413 Dähre, Germany

[*]*Now at Institute for Geography, Universität Augsburg, Alter Postweg 118, 86159, Augsburg, Germany, pedro.batista@~~unibas.ch~~geo.uni-augsburg.de

Abstract

The accelerated sediment supply from agricultural soils to riverine and lacustrine environments leads to negative off-site consequences. In particular, the sediment connectivity from agricultural land to surface waters is strongly affected by landscape patchiness and the linear structures that separate field parcels (e.g. roads, tracks, hedges, and grass buffer strips). Understanding the ~~feedbacks~~ interactions between these structures and sediment transfer is therefore crucial for minimising off-site erosion impacts. Although soil erosion models can be used to understand lateral sediment transport patterns, model-based connectivity assessments are hindered by the uncertainty in model structures and input data. In ~~particular~~specific, the representation of linear landscape features in numerical soil redistribution models is often compromised by the spatial resolution of the input data and the quality of the process descriptions. Here we adapted the WaTEM/SEDEM model using high resolution spatial data (2 m x 2 m) to analyse the sediment connectivity in a very patchy mesoscale catchment (73 km^2) of the Swiss Plateau. ~~Specifically, we~~We used a global sensitivity analysis to explore model structural assumptions about how linear landscape features (dis)connect the sediment cascade, which allowed us to investigate the uncertainty in the model structure. Furthermore, we compared model simulations of hillslope sediment yields from five sub-catchments to tributary sediment loads, which were calculated with long-term water discharge and suspended sediment measurements. The sensitivity analysis revealed that the assumptions about how the road network (dis)connects the sediment transfer from field blocks to water courses had a much higher impact on modelled sediment yields than the uncertainty in model parameters. Moreover, ~~M~~model simulations showed a higher agreement with tributary sediment loads when the road network was assumed to directly connect sediments from hillslopes to water courses. Our results ultimately illustrate how a high-density road network combined with an effective drainage system increases sediment connectivity from hillslopes to surface waters in agricultural landscapes. This further highlights the importance of considering linear landscape features and model structural uncertainty in soil erosion and sediment connectivity research.

1 Introduction

Rainfall events on sloped surfaces continuously displace soil particles, which are transported downslope as sediments. These sediments are then stored and remobilised several times before conceivably reaching surface waters. Accordingly, the sediment cascade is a natural and potentially long geomorphological process (Fryirs, 2013). However, the accelerated sediment supply from agricultural soils to riverine and lacustrine environments leads to negative off-site consequences. Specifically, ~~nutrient~~phosphorus-rich and pollutant-bound particulate matter from arable land is associated to the eutrophication and contamination of water courses (Krasa et al., 2019; Laceby et al., 2021). Extreme erosion events in agricultural fields are also linked to the occurrence of muddy floods (Boardman, 2020) and to damages to downstream infrastructure (Bauer et al., 2019). Therefore, understanding how and when sediment is transferred from agricultural fields to different landscape compartments is imperative to reduce off-site erosion impacts.

The degree with which a system facilitates sediment transfer within its internal compartments is defined by Heckmann et al. (2018) as sediment connectivity. This concept can be further distinguished into a structural component, associated to the semi-static spatial configuration of the landscape; and a functional one, which emerges as a dynamic property of the hydro-sedimentological system (Wainwright et al., 2011). Connectivity theory therefore provides a framework to rethink the sediment delivery problem (Fryirs, 2013; Parsons et al., 2009) and to understand the complex spatio-temporal processes that regulate sediment transport.

In agricultural landscapes, sediment connectivity is strongly affected by the patchiness of the land use configuration, and the presence of linear features between field parcels (e.g. hedges, grass buffer strips, and roads) (Alder et al., 2015; Bakker et al., 2008; Chartin et al., 2013; Fiener et al., 2011; Remund et al., 2021; Van Oost et al., 2000). The importance of landscape patchiness in regulating sediment transfer is specifically relevant in areas where a large number of small fields, separated by linear structures, create a complex hydrological system. However, the experimental analysis of sediment connectivity at catchment scale is challenging, as it involves measuring both internal soil redistribution processes and cascading sediment transport rates. The interaction between landscape patchiness, linear structures, and sediment connectivity is therefore not addressed by the typical setup of experimental erosion studies, which either focus on small erosion plots or catchment sediment yields (Fiener et al., 2019).

Due to the difficulties in measuring the processes that affect sediment movement at catchment and landscape scale, it is common practice to analyse connectivity with modelling approaches (Nunes et al., 2018). These usually rely on high-resolution process-based models, assuming they are able to represent connectivity dynamics (Baartman et al., 2020); semi-qualitative indices (Borselli et al., 2008; Cavalli et al., 2013); or more recently, the coupling of conceptual models with probability theory (Mahoney et al., 2020a, 2020b). In specific, the use of process-based soil erosion and sediment transport models might be an important pathway to improve our understanding of sediment connectivity (Nunes et al., 2018).

However, erosion models in general, and process-based models in particular, face two fundamental problems for representing sediment connectivity : (i) the input data requirements are large and uncertain, and model application is often restricted to small catchments with a maximum size of a few square kilometres (e.g. Baartman et al., 2020; Starkloff and Stolte, 2014; Wilken et al., 2017) and (ii) the implemented process descriptions, especially along linear landscape features and field boundaries, are weakly defined due to the aforementioned unavailability of experimental data. Borrelli et al. (2018) demonstrated how parcel-specific high resolution land cover and management data can improve soil erosion/sediment delivery models in patchy agricultural catchments.

Here, we aimed to (i) adapt a conceptual soil erosion and sediment delivery model with high spatial resolution data (2 m x 2 m) within a Monte Carlo framework; (ii) to analyse the sediment connectivity in a very patchy mesoscale catchment (73 km^2) in Switzerland; and (iii) to perform a sensitivity analysis of model parameters and structural assumptions regarding how linear features (dis)connect the sediment cascade. Hence, we demonstrate how models can be used to understand the interaction between linear features, landscape patchiness, and sediment connectivity. This will contribute to increase our comprehension of relevant connectivity processes and our ability to develop appropriate measures for reducing off-site erosion impacts.

2 Materials and methods

2.1 Study catchment

The study catchment consists of the contributing area of the Lake Baldegg, in the central Swiss Plateau (Figure 1). The lake has been extensively studied due to its hypertrophic waters, which have been artificially oxygenated since 1983 (e.g. Lavrieux et al., 2019; Müller et al., 2014; Teranes and Bernasconi, 2005). The eutrophication of the lake has been mostly linked to excessive phosphorus loads during the 20^{th} century (Wehrli et al., 1997). Although water quality in the lake is currently improving (BAFU, 2016), the supply of phosphorus-rich sediment is still a concern to local authorities (von Arb et al., 2021; Stoll et al., 2019). The major advantage of the Baldegg catchment for this study is that a comprehensive hydrological data set is available based on an ongoing, long-term monitoring by the Department of Environment and Energy of the Canton of Lucerne.

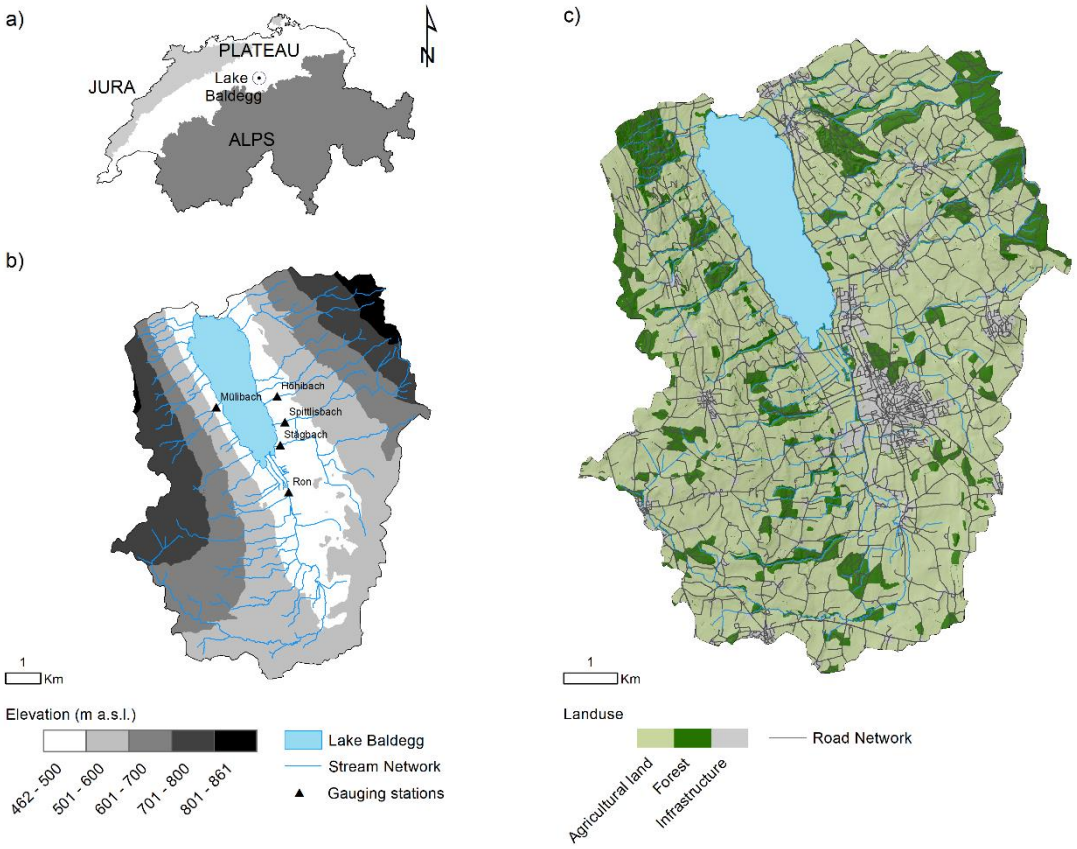

Figure 1. a) Location of the Baldegg catchment; b) elevation, stream network, and location of hydrological gauging stations; c) land use. Data source: Swisstopo~~,~~ (2018, 2020). Sub-catchment areas: Höhibach (2.3 km^2), Mülibach (1.6 km^2), Stägibach (9.3 km^2), Spitllisbach (3.8 km^2), Ron (27.7 km^2).

The Baldegg catchment has a total area of 73.2 km^2, of which 5.2 km^2 are covered by the lake. The remaining area is occupied by agricultural land (74%), forests (16%), and infrastructure (e.g. settlements, developed areas, and roads) (10%) (Swisstopo, 2020) (Figure 1c). The agriculture consists of intensively managed pastures and/or meadows, cereal production under crop rotation, permanent grasslands, fruit orchards, and small vineyards (Lavrieux et al., 2019; Stoll et al., 2019). The majority of the meadows are composed of a mixture of grasses and clover, which are harvested for silage, hay, or barn feeding up to six times per year (von Arb et al., 2021). Agricultural field blocks, here delimited by external boundaries (e.g. roads, water courses, and forests) (Bircher et al., 2019), have a median size of 4.4 ha. However, smaller patches separated by hedges, tree lines, and grass buffer strips, are generally found within the blocks (Figure 2).

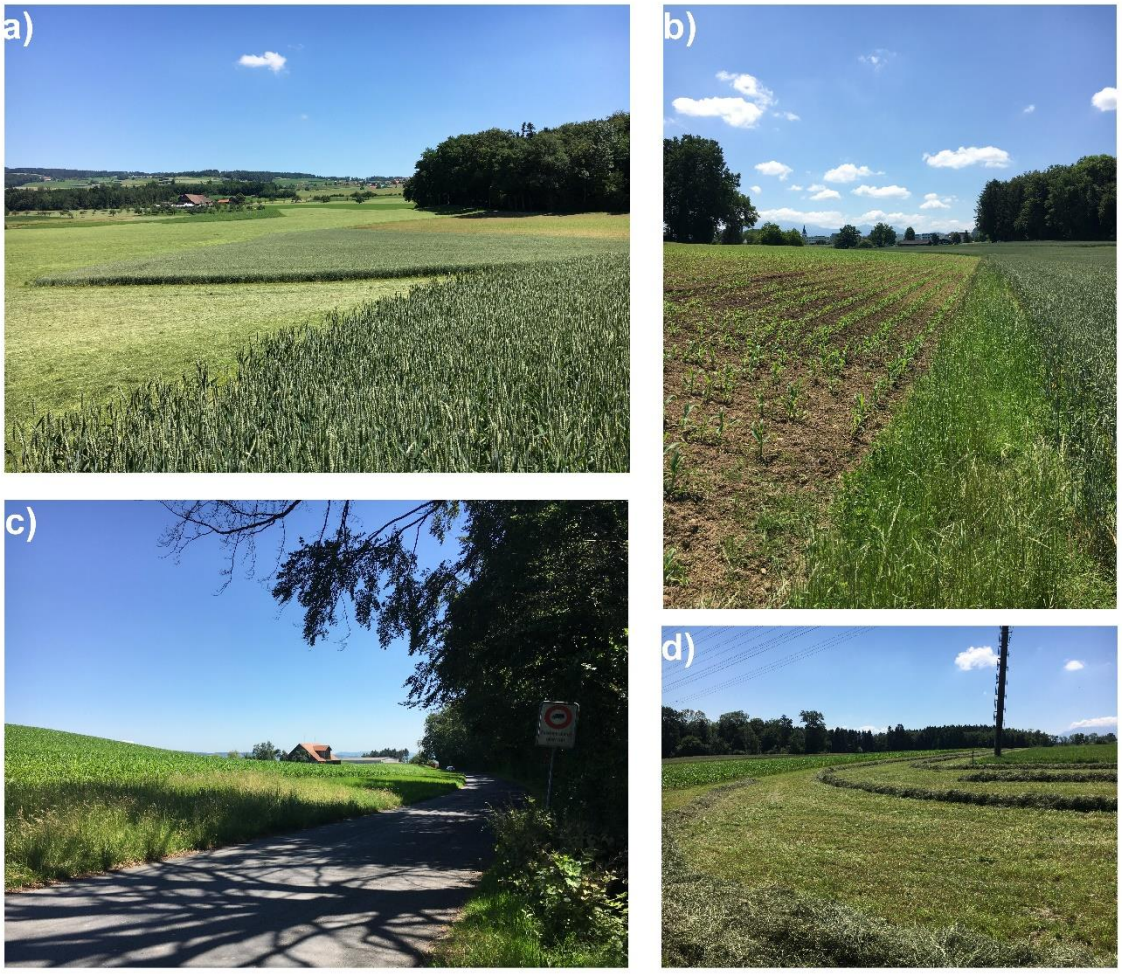

Figure 2. Typical agricultural landscapes from the Baldegg catchment: a) Small arable and grassland patches within larger field blocks, b) grass buffer strip between maize and wheat fields, c) wide grass buffer strip between maize field and a vicinal road, d) freshly cut hay from a pasture ~~in~~ between maize fields.

The road network density in the Baldegg catchment is 6.0 km km^{-2}, which is approximately three times higher than the stream density (1.9 km km^{-2}). Streams in the upper catchment are often incised, with visible, yet not prominent, signs of bank erosion. A total of 22 channels flow into the Lake Baldegg, of which five streams are monitored for water and sediment discharge by cantonal authorities, as described in section 2.2.

The elevation in the Baldegg catchment ranges from 462 to 861 m a.s.l. Steeper slopes (average values above 10°) and higher altitudes are found in the eastern and western sides of the catchment (Figure 1b), in a typical glacial landscape of the Swiss Plateau – in this case formed by the retreat of the Reuss Glacier in the south to north direction (~18,000 years BP) (Keller, 2021; Pfiffner, 2021). As a result, calcaric Cambisols (IUSS Working Group WRB, 2006) developed upon Tertiary and Quaternary

deposits are the main soil class in the catchment. Rainfall is well distributed throughout the year, although greater precipitation is observed from May to August. The average annual rainfall (2010-2019) at the closest gauging station is ~ 1000 mm yr^{-1} (Mosen, 454 m a.s.l., ~3.5 km north of the Lake Baldegg, acquired from MeteoSwiss 2021) and mean rainfall erosivity in the catchment is ~ 1150 MJ mm ha^{-1} h^{-1} yr^{-1} (Schmidt et al., 2016).

2.2 Tributary suspended sediment loads

Suspended sediment concentrations from five tributaries to the Lake Baldegg are monitored by the Department of Environment and Energy of the Canton of Lucerne. Here, we used the data measured from Jan 2010 to Dec 2019. On average 274 grab samples were taken from each tributary, which corresponds to one sample every 22 days, ~~plus additional~~in addition to the samples collected during high-flow events (10 – 13 per year) (Figure 3). Suspended sediments were measured at the same location where water discharge was monitored by automatic gauging stations (Figure 1b). A summary of the measured rainfall, water discharge, and sediment concentration from 2010 to 2019 is displayed in Figure 3.

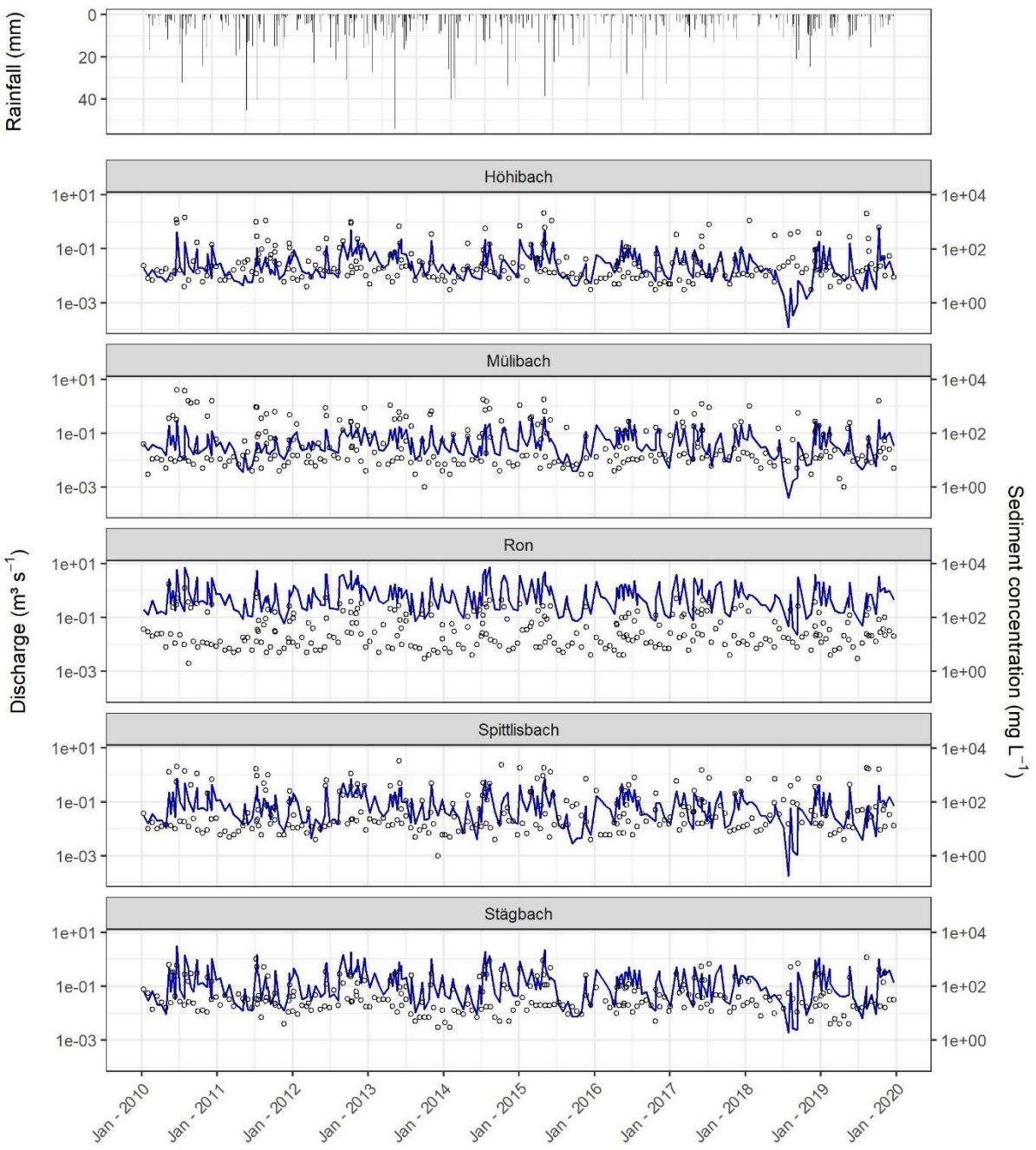

143

144 Figure 3. Daily rainfall at the Mosen station, mean daily discharge (blue line), and sediment
145 concentration (circles) at the monitored tributaries of the Lake Baldegg (2010-2019). Data source:
146 MeteoSwiss (2021).

In order to ~~calculate~~ estimate continuous daily sediment concentration values, later used to produce average yearly sediment loads for each tributary, we used a rating curve approach (Equation 1), combining the roughly triweekly sediment concentration measurements with continuous discharge measurements. The rating curve partially accounts for hysteresis and seasonality (Table 1), which can have a significant impact on sediment export patterns and reflect the catchment landuse, hydrological connectivity, and internal sediment source dynamics (Sherriff et al., 2016). To derive the coefficients in Equation 1 we used a parsimonious multivariate regression which does not require separate calibration for different seasons (Cohn et al., 1992; Vigiak and Bende-Michl, 2013).

~~the sediment load for the monitored tributaries, we fitted a rating curve (Equation 1) with the measured sediment concentrations and their correspondent discharge. Additional covariates were included to account for hysteresis, seasonality, and constituent exhaustion (Table 1) (Vigiak and Bende-Michl, 2013; Wang et al., 2011):~~

$$\ln c_i = \beta_0 + \sum_{k=1}^{5\text{~~4~~}} \beta_k x_{k,i} + \varepsilon_i \quad (1)$$

Where: c is sediment concentration (mg L^{-1}) for day i, β_0 is the intercept, β_k are fitted coefficients, $x_{k,i}$ are covariates (Tab. 1) accounting for discharge, hysteresis, and seasonality ~~and constituent exhaustion~~, k is the covariate identification, and ε_i is the residual error.

Table 1. Covariates used for fitting the sediment-rating curves, as in Vigiak and Bende-Michl (2013). ~~and Wang et al. (2011).~~

Covariate	Expression	Explanation	Physical interpretation
$x_{1,k}$	$\ln Q_i$	Q_i = discharge for day i (m^3s^{-1})	Discharge
$x_{2,k}$	$(\ln Q_i)^2$	Quadratic term of $x_{1,i}$	Hysteresis
$x_{3,k}$	$\sin(2\pi M_i/12)$	M_i = month of day i	Seasonality
$x_{4,k}$	$\cos(2\pi M_i/12)$	M_i = month of day i	Seasonality
~~$x_{5,k}$~~	~~$\frac{\sum_{z=1}^{i} 0.95^{i+1-z} Q_z}{\sum_{z=1}^{i} 0.95^{i+1-z}}$~~	~~Discount flow up to day i~~	~~Constituent exhaustion (see Wang et al., 2011)~~

~~The rating curve was used to estimate daily sediment concentrations for the entire 2010-2019 period. Subsequently, we propagated~~To analyse the uncertainty in the regressions ~~fit by simulating~~ we simulated posterior distributions of the model coefficients (β_0, β_k) with an informal Bayesian function of the R package '*arm*' (Gelman and Hill, 2007), as in Batista et al. (2021). This function produces realisations of model coefficients based on the residual standard error of the regression, which means that models with poorer fits will yield broader posterior distributions of regression coefficients. The

posterior distributions were used to simulate 1000 sediment concentration values for each day *i*. These were transformed into daily distributions of sediment loads (Mg), considering the mean daily discharge measurements from the gauging stations. Sediment loads were ultimately aggregated into average annual values (Mg yr^{-1}) with uncertainty bands, which should allow for a general comparison with the different sediment connectivity scenarios simulated by WaTEM/SEDEM.

2.3 Model description

A modified version of the spatially distributed erosion and sediment transport WaTEM/SEDEM (Van Oost et al., 2000; Van Rompaey et al., 2001; Verstraeten et al., 2010) was used in this study. WaTEM/SEDEM provides a framework for modelling sediment connectivity from hillslope to water courses by use of a steady state transport capacity equation and a pixel-based sediment routing component. That is, the model assumes that soil particles displaced by water erosion at a given grid cell are transferred downstream for as long as the runoff transport capacity is greater than the sediment supply, or until the flow path reaches a definite sink. Although the model is able to simulate both tillage and water erosion, here we focus on the latter, which is calculated with an adaptation of the RUSLE (Renard et al., 1997) (Equation 2). We chose to focus on soil erosion by water because in WaTEM/SEDEM the sediment supply/routing is not affected by tillage erosion. However, tillage erosion is likely to be an important within-field soil redistribution process in the catchment (please see the discussion below). The model is by default executed in an average yearly time step, as typical in RUSLE applications, which predict long-term (~20 years) average annual soil losses:

$$A = R\ K\ LS_{2d}\ C\ P \quad (2)$$

Where: *A* is average annual soil loss (kg m^{-2} yr^{-1}), *R* is rainfall erosivity (MJ mm m^{-2} h^{-1} yr^{-1}), *K* is soil erodibility (kg h MJ^{-1} mm^{-1}), LS_{2d} is a topographic factor calculated by the Desmet and Govers (1996) procedure (dimensionless), *C* is a cover-management factor (dimensionless), and *P* is a support practice factor (dimensionless).

Transport capacity (kg m^{-1} yr^{-1}) per unit widths of grid cells is assumed to be proportional to the potential to rill erosion, which is described by a power function of slope length and gradient (Van Rompaey et al., 2001):

$$TC = K_{TC} RK(LS_{2d} - 4.12\ S_g^{0.8}) \quad (3)$$

Where: K_{TC} is a landuse-dependent transport capacity coefficient (m) which requires calibration, R is rainfall erosivity (MJ mm h^{-1} yr^{-1}), K is soil erodibility (t h MJ^{-1} mm^{-1}), LS_{2d} is a topographic factor calculated by the Desmet and Govers (1996) procedure (dimensionless), and S_g is slope gradient (m m^{-1}).

WaTEM/SEDEM partially incorporates the influence of the landscape structure on sediment transfer by the use of a parcel connectivity parameter P_{Con}, which represents the proportion of sediment that is stopped at field borders. The model also simulates runoff connectivity by means of a parcel trapping efficiency P_{TEf} parameter, which corresponds to the proportion of the flow accumulation that is routed downstream. Finally, the model is able to estimate the total amount of sediment transferred from hillslopes to water courses, which can be interpreted as the hillslope component of a catchment sediment budget. Since WaTEM/SEDEM does not represent gully and bank erosion, nor in-stream erosion and deposition processes, any comparison between modelled sediment yields and catchment-outlet sediment loads must be interpreted with caution. However, in catchments where rill and interrill are the main overland erosion processes, and assuming a state of long term fluvial quasi equilibrium, the outlet sediment loads should be at least comparable to the model outputs – even if not fully commensurable. For further information on the model, we refer to Notebaert et al., (2006), Van Oost et al., (2000), Van Rompaey et al., (2001), and Verstraeten et al., (2010).

2.4 Model implementation, input data, and sensitivity analysis

WaTEM/SEDEM is ~~–~~implemented as a ~~user-friendly~~user-friendly GUI developed at KU Leuven (Notebaert et al., 2006). Although the software facilitates model application, it does not allow for more complex operations, such as sensitivity or uncertainty analysis. Moreover, some model components might not be fully comprehensible without access to the source code, and WaTEM/SEDEM is frequently used as a black box. Hence, in order to perform a sensitivity analysis of model parameters and underlying structural model assumptions, we implemented a WaTEM/SEDEM version using the free open source software R (R Core Team, 2021) and SAGA GIS (Conrad et al., 2015). The main adaptations are described in the following, and our code is available as supplementary material.

Our model application consists of a global all-at-a-time sensitivity analysis, as described by Pianosi et al. (2016). That is, we performed a Monte Carlo simulation to explore the variability of the whole parameter space, and all input factors were sampled simultaneously for each model realisation (n = 1200). The framework is similar to an uncertainty analysis, except in this case we did not focus on locating the parameter space which produced behavioural model realisations. Instead, we concentrated on apportioning sources of uncertainty to different model input factors, aiming to rank their contribution to the variability of the response surface (see Pianosi et al., 2016 for a review on sensitivity analysis). This should allow us to identify parameters and model assumptions that have a greater impact on the manner with which WaTEM/SEDEM describes sediment connectivity in the Baldegg catchment. In particular, the analysis of different assumptions about the structure of the model should provide a

connectivity assessment based on the quantification of the structural uncertainty within the simulations. To the best of our knowledge, this is the first time the analysis of model structural error is incorporated to sediment connectivity research.

For each iteration of the Monte Carlo simulation, ~~all~~ RUSLE input variables were sampled from uniform distributions~~, except for the LS_{2d} factor~~ (Table 2). Minimum and maximum *R* factor values were retrieved from the Swiss national map (Schmidt et al., 2016), and a single lumped value for the whole catchment was sampled for each iteration. The same approach was used for the *K* factor (Schmidt et al., 2018a). We used lumped catchment values for these factors due to their low spatial variability within the study area, according to the national maps (coefficient of variations are 1% and 7% for the *K* and *R* factor, respectively). For the *C* and *P* factors, here combined in a single *CP* parameter, uniform distributions were created for each landuse class in the catchment, based on commonly used values from the literature and a land cover map (1:25000) (Swiss Map Vector 25 BETA~~Swisstopo, 2020~~) (Swisstopo, 2018), which we rasterised to the model resolution (2 m x 2 m). ~~Due to the unavailability of open source geodata of crop statistics in the Baldegg catchment~~Due to the difficulties involved in accurately representing long-term average agricultural landuse patterns and farming management practices per field parcel, pastures and cropland were ~~aggregated~~ considered ~~into~~ a single arable land category, using only the information available from the land cover map (Table 2) (Swiss Map Vector 25 BETA) (Swisstopo, 2018). In this case, minimum and maximum values were relaxed to represent a wide possible combination of crops and support practices. Such combinations were assessed with the *CP*-Tool (Kupferschmied, 2019), which allows for the calculation of *CP* values considering common crop rotation systems in Switzerland. The minimum *CP* values were particularly reduced to include typical values for permanent grasslands in Switzerland (~0.01) (Schmidt et al., 2018b). This simplified approach should be appropriate considering i) our focus on connectivity scenarios and linear landscape structures, and ii) the use of the Monte Carlo simulation with the sampling of a wide parameter space that accounts for the uncertainty in the landuse classification. Finally, the LS_{2d} factor was calculated with a slope (rad) and an upslope contributing area (m^2) grid, which were obtained by processing a 2 m x 2 m resolution DEM from SwissALTI3D (Swisstopo, 2014a). In this case, the error in the LS_{2d} factor was not incorporated into Monte Carlo simulation due to the use of the high-resolution DEM, which should considerably reduce the uncertainty associated to the parameter estimation.

Table 2. Minimum and maximum parameter values sampled during the Monte Carlo simulation.

Parameter	Category	Min	Max
R (MJ mm m^{-2} h^{-1} yr^{-1})		950 10^{-4}	1350 10^{-4}
K (kg h MJ^{-1} mm^{-1})		0.025 10^{3}	0.040 10^{3}
CP (-)	Arable land	0.01	0.5
	Grass buffer strips	0.001	0.009
	Forest	0.0001	0.003
	Orchard	0.001	0.2
	Vineyard	0.05	0.6
K_{TC} (m)	High (arable land, vineyard)	1	200
	Low (grass buffer strips, forest, orchard)	1	100
P_{TEf} (-)		0	1
P_{Con} (-)		0	1

Similarly, all WaTEM/SEDEM-specific model parameters were sampled from uniform distributions (Table 2). Landuse classes with a *CP* factor above 0.01 received higher transport capacity coefficients (K_{TC} high). The remaining landuse classes, namely forests and grass strips, received lower coefficients (K_{TC} low). The K_{TC} reference values were taken from Van Rompaey et al. (2001) and extended in order to explore a larger parameter space. The sampled parcel trapping efficiency (P_{TEf}) values were assigned to forests and grass buffer strips in the rasterised land cover map, as we explain below. The resulting P_{TEf} grid was used as a weight for calculating the aforementioned upslope contributing area. Hence, only a proportion of the grid-cell area from forests and grass strips contributed to the downstream flow accumulation, as runoff amounts are assumed not to increase (or to increase slowly) with slope length under natural vegetation (Govers, 2011). Parcel connectivity (P_{Con}) values were assigned to the forest and grass buffer strips cells that bordered agricultural fields, representing the extent with which water and sediment transport is reduced at parcel borders (Notebaert et al., 2006). The transport capacity (Eq. 2) at these cells was reduced by a fraction inversely proportional to the sampled P_{Con} value.

For each sampled combination of parameters values, the models were ~~ran~~ applied with and without the presence of grass buffer strips between agricultural field blocks and adjacent roads and forests. Although grass buffer strips are generally present at field borders in the Baldegg catchment (Figure 2), these features were not distinguishable in the land cover map. Hence, we manually inserted 2 m wide grass buffer strips at the aforementioned borders. The extent of the buffer-strips in reality is quite variable, and generally wider at forest and river vicinities (3 – 6 m), as required by law in Switzerland (Alder et al., 2015). For simplicity, we used a single value that should allow us to test the sensitivity of the model to the presence of the strips. The 2 m width was selected based on the spatial resolution of the model input data. ~~On the other hand, h~~Hedges and tree lines within field blocks were already classified in the ~~land cover map~~large-scale topographic landscape model of Switzerland (swissTLM3D) (Swisstopo, 2020) and required no additional processing apart from a merge with the land cover map (Swiss Map Vector 25 BETA) (Swisstopo, 2018).

Furthermore, three road connectivity assumptions were assessed for each model iteration. For such, we first converted the roads from polylines (as available in the swissTLM3D) to polygons, using a buffer distance based on the road widths. Next, these polygons were rasterised and incorporated into the land cover grid used for modelling. In a first scenario, roads were treated as an ultimate sink, with zero transport capacity (i.e., 'roads as sinks'). Hence, sediments reaching roads or infrastructure were subsequently removed from the system and did not reach surface waters. This represents a scenario in which roadside ditches and the road drainage system trap most sediments and partly diverge runoff to wastewater treatment plants. A second scenario assumed that all sediments reaching the road network were directly connected to the stream network. This represents a situation in which the road drainage system acts as a hydraulic shortcut, transferring sediments from fields into surface waters (i.e., 'roads as shortcuts') (see Schönenberger and Stamm, 2021). As in the original model formulations (see Notebaert et al., 2006), the third scenario assigned very high transport capacity to roads and infrastructure, so that no deposition would take place (i.e. 'roads as patch connectors'). In this case, runoff and sediment might flow along or across the road network – which is expected to happen during extreme rainfall events when the drainage system is clogged. For this scenario, deposition will never occur on road cells, however sediments can still be deposited on lower patches before reaching the stream network. Hence, sediment transfer will be entirely dependent on the flow direction calculated from the DEM. Here we employed a multiple flow direction algorithm, which was used for calculating upslope contributing area and routing sediments along the flow path. The sediment routing component was implemented with a capacity accumulation function from SAGA GIS (Conrad et al., 2015), and all geo-processing tools were applied with the 'RSAGA' package (Brenning et al., 2018).

The sensitivity of WaTEM/SEDEM to the uncertainty in model parameters, the presence of grass buffer strips, and assumptions about road connectivity (i.e., model structural uncertainty) was assessed by evaluating modelled hillslope sediment yields (i.e., the amount of sediment delivered from hillslopes to surface waters) for the entire Baldegg catchment. A qualitative analysis was performed with a visual inspection of scatter plots, comparing the univariate parameter space with the model response surface. Additionally, we used a random forest analysis (RFA) to rank the importance of input factors to the uncertainty in model outputs (Antoniadis et al., 2021). That is, a random forest was used to predict the WaTEM/SEDEM-modelled sediment yields, based on the sampled parameter values for each iteration of the Monte Carlo simulation. The importance of the input factors, including model parameters, the presence of grass -strips, and the road connectivity scenarios, was ranked based on their relative contribution to the RFA predictive error, following an out-of-bag estimate (Breiman, 2001). We chose the RFA due to its ability to rank both qualitative and quantitative input factors. The analysis was performed with the 'randomForest' (Liaw and Wiener, 2002) R package.

Finally, we compared the resulting WaTEM/SEDEM simulations of sub-catchment hillslope sediment yields to the suspended sediment loads from the monitored tributaries. Of note, with this comparison we

only aim to provide a general picture of the plausibility of the model realisations. Suspended sediment loads are a product of a complex interaction of hillslope and channel remobilisation processes, which are not fully represented by WaTEM/SEDEM. In addition, since the model is RUSLE-based, the soil redistribution rates represent long-term average annual values, which hampers a straightforward comparison with annual sediment transport rates. Hence, modelled hillslope yields and suspended loads are not entirely commensurable, and we did not focus on a rejectionist framework for model testing. This research is exploratory and investigates the importance of linear features and landscape patchiness on sediment connectivity.

3 Results

3.1 Sensitivity analysis

The road connectivity assumptions were by far the most sensitive input factor for WaTEM/SEDEM in the Baldegg catchment. This is illustrated in Figure 4, which presents scatter plots comparing sampled parameter values and the model response surface. The uniformly scattered points denote a low sensitivity of the modelled hillslope sediment yields to most input factors, with some evident exceptions: *CP* for arable land, K_{TC} high, and K_{TC} low. On the other hand, all plots demonstrate that higher sediment yields were calculated when we assumed that roads behaved as hydraulic shortcuts, directly connecting agricultural patches to the stream network.

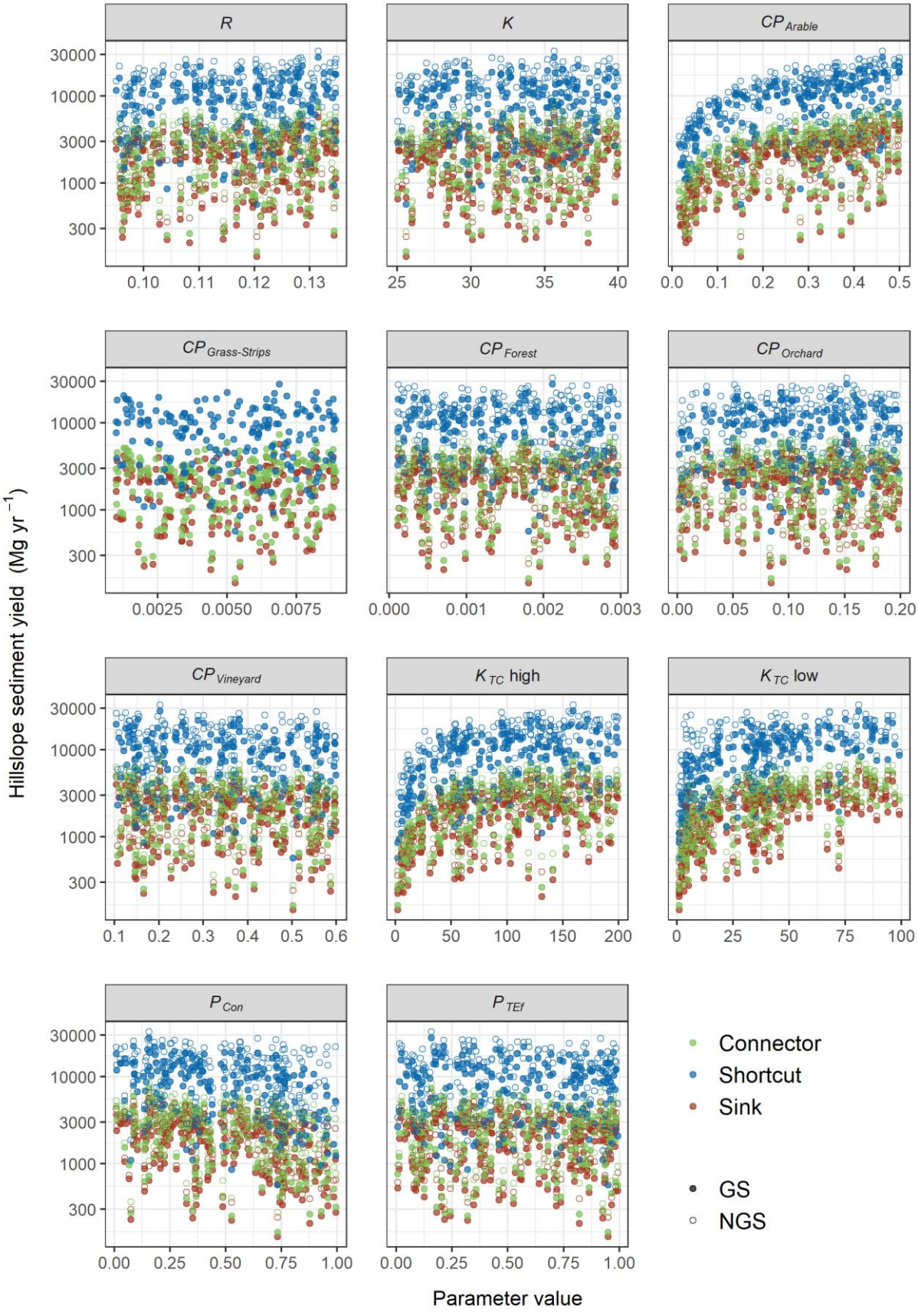

Figure 4. Univariate scatter plots of sampled parameter values. Full circles represent model realisations with the presence of grass buffer strips (GS), and open circles represent the ones without strips (NGS).

Colours represent the road connectivity assumptions (i.e. ‘roads as patch connectors’, ‘roads as hydraulic shortcuts’, and ‘roads as sinks’). See section 2.4 for a description of road connectivity scenarios.

Similarly, the results from the RFA demonstrate that road connectivity was the most important input factor for predicting the WaTEM/SEDEM outputs (Figure 5). That is, if road connectivity was not considered, the predictive mean squared error (MSE) of the RFA increased by ~~158~~265%. The MSE increase associated to *CP* for arable land (~~72~~96%), K_{TC} low (~~35~~51%), K_{TC} high (~~34~~45%), and the presence of grass buffer strips (~~11.0~~33%), indicate the model was also sensitive these input factors. However, if we considered each road connectivity scenario individually, the results from the random forest were shifted, as the model seemed to be more sensitive to the presence of grass buffer strips for the 'road as shortcuts' scenario (MSE increase = ~~65~~55%).

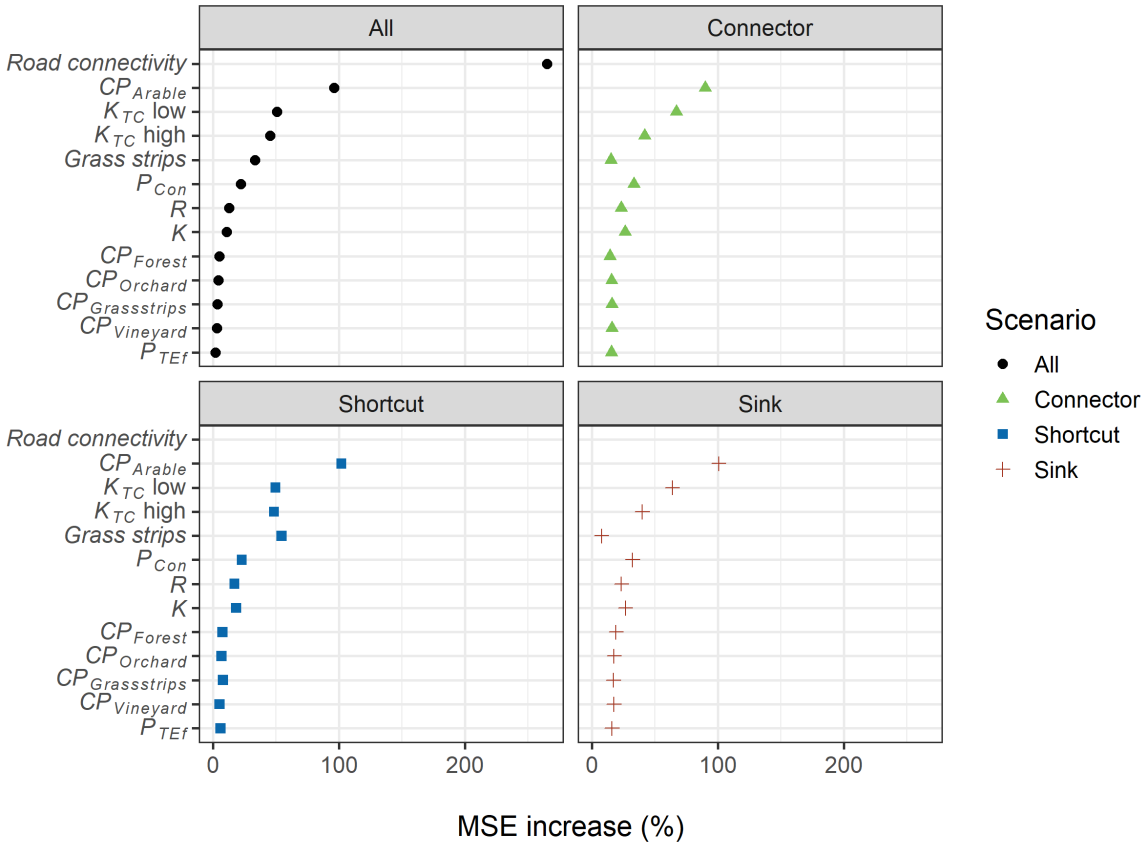

Figure 5. Mean squared error (MSE) increase associated to model input factors for the ~~RFA~~Random Forest Analysis (RFA). Larger relative errors indicate the input factors were more important for estimating model outputs.

3.2 Spatial patterns

The spatial patterns of soil redistribution rates were also highly influenced by linear features, landscape patchiness, and connectivity assumptions. Sediment deposition on field blocks downslope from roads was more frequently observed for the 'roads as connectors' scenario, than for the other road connectivity assumptions. Specifically, when sediments were not diverged or trapped by the road network, there was

370 a greater proportion of sediment deposition on footslope field borders and other potential sinks (Figure
371 6b) (Table 3).
372

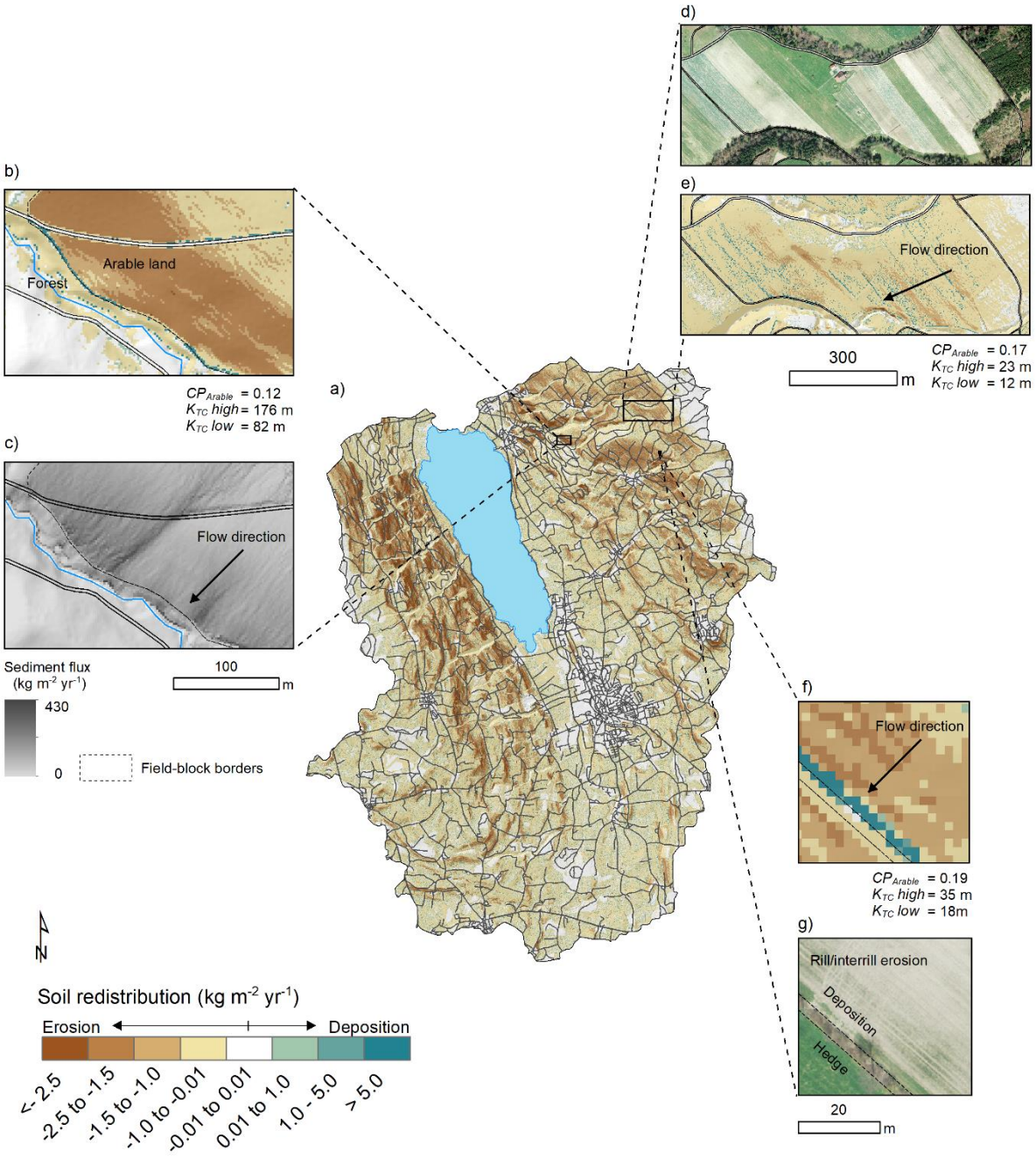

Figure 6. a) Catchment patterns of soil redistribution for a model realisation with the presence of grass buffer strips; b) detail of sediment deposition on field borders, 'road as patch connectors' scenario; c) detail of sediment fluxes across the road network, 'road as patch connectors' scenario'; d) detail of aerial image of multiple parcels within a field block (Swisstopo, 2014b); e) soil redistribution rates for the field block; f) detail of sediment deposition at a grass buffer strip at a field border; g) aerial image for the field (Swisstopo, 2014b).

The sediment flux from agricultural fields was generally interrupted when entering forest patches, and further deposition was modelled at forested valley floors, near the stream channels, for all scenarios (Figure 6b, c). Importantly, sediment deposition along grass buffer strips, hedges, and tree lines reduced sediment fluxes in between field blocks, forming a patchy connectivity pattern. This was again visible for all simulated connectivity assumptions, albeit particularly pronounced when the presence of grass buffer strips was considered (Figure 6 a, f).

Unexpectedly, the soil redistribution patterns revealed that WaTEM/SEDEM simulated linear deposition areas at the borders of small cropland patches (Figure 6d, e). This occurred even in the absence of grass buffer strips or hedges, and hence without P_{Con} parameterisation, which was only applied to field-block borders. These depositional patterns were particularly evident within field blocks oriented across the slope direction, and apparently stem from small scale changes in the slope gradient, which were represented by the high-resolution DEM and which potentially results from long-term tillage erosion.

3.3 Soil redistribution rates, hillslope sediment-yields, and suspended sediment loads

Soil redistribution rates for eroding grid cells in the Baldegg catchment were almost identical among the simulated road connectivity assumptions (Table 3). Higher absolute deposition rates were calculated for the simulations without grass strips for both the connector and sink scenarios, which is a result of increased erosion rates calculated without the presence of the strips. On the other hand, lower sediment yields were calculated with the presence of grass buffer strips when the connectivity scenarios were analysed individually. Among these scenarios, deposition rates were lower if roads were considered to behave as hydraulic shortcuts. Contrarily, deposition rates for the 'roads as connectors' and 'roads as sinks' scenarios were very similar, although road deposition was only modelled in the second case. Therefore, deposition rates within fields, patch borders, colluviums, and valley floors for the connector scenario were ~30% higher than for the other simulations. As the sediments not diverged by the road network were ultimately deposited within the catchment, the sink and connector scenarios displayed very similar hillslope sediment yields. Contrarily, sediment yields for the shortcut scenario were in general ~4.5 times higher than for the remaining road connectivity simulations.

Table 3. Summary statistics of soil redistribution rates, hillslope sediment yields calculated by the WaTEM/SEDEM simulations.

Scenario		Erosion			Deposition			SSY			SY		
		---------- Mg ha^{-1} yr^{-1} ----------									--------- Mg yr^{-1} ---------		
		Q1	Q2	Q3	Q1	Q2	Q3	Q1	Q2	Q3	Q1	Q2	Q3
Connector	GS	3.5	6.3	8.7	3.4	5.9	8.3	0.2	0.3	0.5	1,047	2,248	3,307
	NGS	3.7	6.6	9.1	3.5	6.1	8.5	0.2	0.4	0.6	1,498	3,054	4,097
Shortcut	GS	3.5	6.3	8.8	2.7	4.9	7.2	0.6	1.2	1.8	3,878	8,467	12,242
	NGS	3.7	6.6	9.2	2.5	4.7	6.7	0.9	1.9	2.6	6,303	13,238	17,506

Sink	GS	3.5	6.3	8.8	3.4	6.0	8.4	0.1	0.3	0.4	833	1,828	2,665
	NGS	3.7	6.6	9.2	3.5	6.2	8.7	0.2	0.4	0.5	1,143	2,389	3,197

SSY: area specific hillslope sediment yield; SY: hillslope sediment yield. Deposition rates include hillslope and road deposition. GS: grass buffer strips; NGS: no grass buffer strips; Q1: first quartile, or the 25th percentile; Q2: second quartile, or the median; Q3: third quartile, or the 75th percentile.

The comparison between WaTEM/SEDEM simulations and the~~–~~ tributary sediment loads revealed a larger overlap between the latter and the results from the 'road as shortcuts' scenario (Figure 7). The overlap became particularly clear when we compared the prediction intervals of the calculations (Figure 7). That is, a smaller proportion of the 'road as connectors' and the 'road as sinks' model realisations encompassed the tributary sediment loads, except for the Höhibach, which showed the opposite pattern. This behaviour was particularly evident for the scenario with the presence of grass buffer strips.

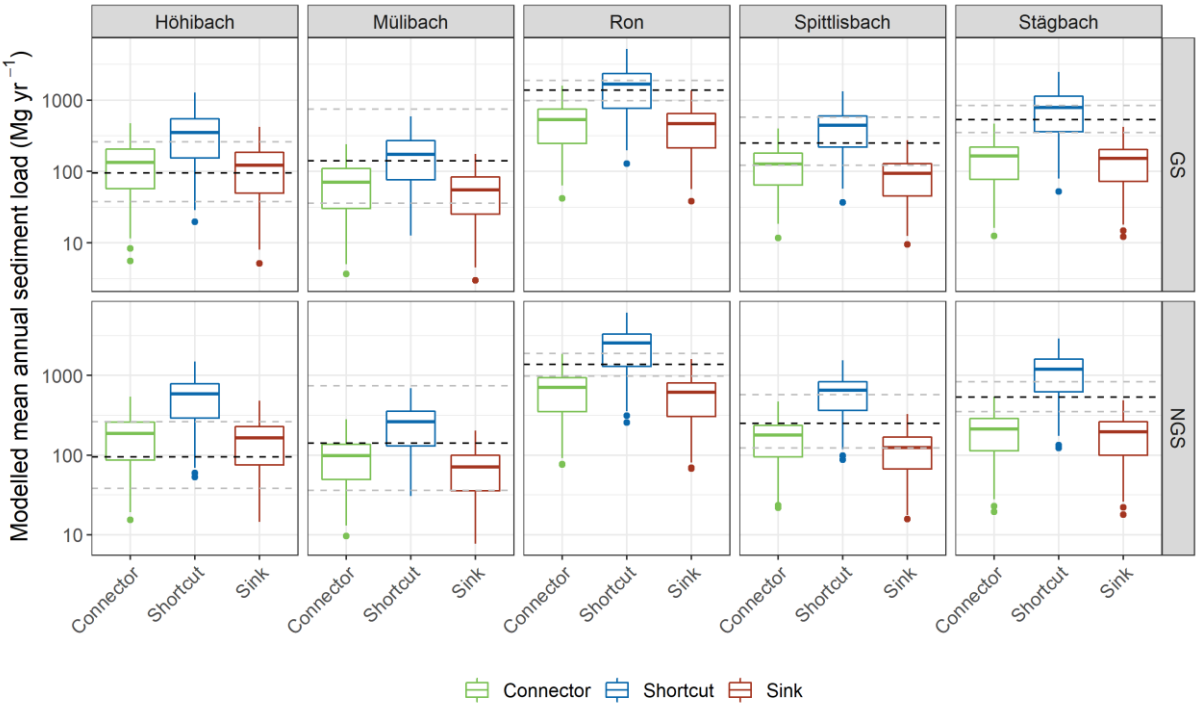

Figure 7. Box-plots of hillslope sediment loads simulated by WaTEM/SEDEM for the road connectivity scenarios for each tributary sub-catchment. Dashed lines represent the median (in black) and the 95% interval (in grey) of the measurement-based estimates of sediment loads for each tributary, calculated from the error propagation of the sediment-rating curve. GS: grass buffer strips, NGS: no grass buffer strips. Simulations for the shortcut scenario generally shows a higher overlap with calculated sediment loads, in particular when grass buffer strips are considered.

It is important to note that the median daily sediment concentrations calculated ~~by~~ from the 1000 realisations of the rating curves (Equation 1) underestimated the ~~actual observations~~high sediment concentration measurements, for all tributaries. This ~~is expressed by~~resulted in the positive mean error of the median estimates (Table 4). Moreover, the Nash-Sutcliffe model efficiency coefficient for the median calculations was unsatisfactory considering the usual thresholds for model performance (e.g.

Moriasi et al., 2015). ~~On the other hand~~However, the 95 % prediction interval of the rating curves encompassed a large proportion of the sediment concentration observations for the tributaries with poorer fits and wider uncertainty bands (i.e., the Höhibach, Mülibach, and Spittlisbach) (Table 4, Supplementary Material Figure 1)~~, and most errors were associated to extreme events (Table 4, Figure 8)~~. The sediment rating curves for the tributaries which displayed a better fit (i.e., the Ron and Stägbach) encompassed a much lesser proportion of the observed sediment concentration values (Table 4, Supplementary Material Figure 1). That is, the regressions with the lowest residual standard errors had narrower uncertainty bands, which albeit produced more accurate median predictions, led to a greater proportion of observations out-of-bound from the 95 % prediction interval. In any case, the largest errors were associated to underestimates of extreme events, and therefore, ~~Hence,~~ it is likely that actual sediment loads from the tributaries are contained within the long right side of the skewed distributions resulting from the error propagation of the rating curves (Figure 7), which would increase the overlap with the shortcut scenario.

Table 4. Evaluation metrics of the sediment rating curve, considering the measured sediment concentrations and median of the simulations.

Stream	ME	RSME	Out-of-bound percentage*	r_p	r_s	NSE
	----- mg L^{-1}-----		--------- % ---------	----------		
Höhibach	56.58~~50.10~~	80.51~~80.60~~	13~~13~~	0.51~~0.52~~	0.61~~0.64~~	0.20~~0.22~~
Mülibach	96.17~~72.97~~	142.96~~138.32~~	14~~11~~	0.56~~0.64~~	0.72~~0.73~~	0.24~~0.34~~
Ron	24.18~~22.00~~	55.42~~54.61~~	7~~5~~1	0.62~~0.63~~	0.76~~0.77~~	0.35~~0.38~~
Spittlisbach	108.84~~95.67~~	155.85~~149.78~~	29~~22~~	0.46~~0.51~~	0.63~~0.67~~	0.14~~0.20~~
Stägbach	33.88~~25.05~~	68.46~~67.14~~	5~~1~~36	0.47~~0.50~~	0.68~~0.70~~	0.15~~0.19~~

*percentage of observations out of the 95 % prediction interval. ME: mean error; RMSE: root-mean-square error, r_p: Pearson's correlation coefficient, r_s: Spearman's correlation coefficient; NSE: Nash-Sutcliffe model efficiency coefficient.

~~Figure 8. Log-scaled daily sediment concentrations estimates from the rating curve: dark solid line is the median of the calculations and the shaded light blue represents the 95 % prediction interval. Open circles are the observed values used for fitting the curve.~~

4 Discussion

Here we assessed the interaction between landscape patchiness, linear structures, and sediment connectivity. Our quantitative model-based approach highlighted the importance of roads in (dis)connecting sediment fluxes between landscape compartments and surface waters in patchy

agricultural catchments. These findings are in lines with long-term field observations and qualitative model assessments for similar areas in Switzerland.

For instance, Ledermann et al. (2010) monitored off-site erosion in multiple fields from different regions of the Swiss midlands and found that linear features in general and roads in particular had a large influence on runoff concentration, soil erosion rates, and off-site damage. These authors also estimated that > 50 % of eroded soil was deposited in adjacent fields and infra-structure, while up to 20 % reached surface waters, mainly through indirect inflow via the road and drainage network. Such figures are proportionate to WaTEM/SEDEM ~~estimations~~ simulations for the Baldegg catchment, specifically for the shortcut scenario with the presence of grass buffer strips (Table 3). Another interesting similarity between our outputs and the field assessments from Ledermann et al. (2010), was that both approaches identified field border structures as critical regulators of soil erosion and sediment transport (see Figures 5 and 6). According to the field assessments, border furrows are specifically important for both triggering erosion and promoting diffuse sediment deposition. Such features, combined with long-term tillage erosion, might be responsible creating the topographic pattern displayed in Figure 6d.

Moreover, the capacity of roads to connect runoff and sediments from arable land to surface waters in Switzerland was extensively described by Alder et al. (2015) and Schönenberger and Stamm (2021). Both studies used a similar semi-qualitative modelling approach for identifying agricultural fields that were directly or indirectly (i.e. via the road and drainage networks) connected to surface waters. In particular, Schönenberger and Stamm (2021) mapped the location of drainage inlets in multiple small catchments of the Swiss Plateau. Accordingly, these authors identified the road drainage system as the main hydraulic shortcut connecting fields to water courses, as most drainage inlets discharge into surface waters (87%), and only a small proportion of them flow into wastewater treatment plants or depositional areas. Hence, the fact that the WaTEM/SEDEM 'road as shortcuts' scenario displayed a greater agreement with the sediment rating curves for the Baldegg tributaries (Figure 7) is coherent with the current understanding of runoff dynamics in the Swiss Plateau. Of note, the contrasting results for the Höhibach sediment loads (Figure 7), which are much closer to the sink and patch-connector simulations, do not seem to be explained by any physiographical characteristic of the sub-catchment ~~(e.g. stream and road density, slope, or land cover)~~(Supplementary Material Table 1). Hence, we speculate that this different pattern could be caused by a lower inlet drainage density or ~~cropping specificities~~specific farming practices ~~in~~ within the Höhibach contributing area.

In addition, our simulations of edge-of-field grass buffer strips indicated that these structures might be particularly relevant for the 'road as shortcuts' scenario. In this case, the model estimated that grass trips could reduce up to 30% the sediment connectivity from hillslopes to surface waters in the Baldegg catchment (Table 4). However, ~~it should be noted that we~~ we assumed 2 m wide strips at field block borders, irrespectively of the adjacent structures or land use. As previously mentioned, the extent of these features is in fact quite variable, and legislation only requires 0.5 m filters between fields and

roads, as reported by Alder et al. (2015). These authors further emphasised that albeit edge-of-field strips are an important complementary management practice, their effectiveness is often reduced in case of large drainage areas, in which very wide buffers would be necessary to stop sediment fluxes. Hence, Alder et al. (2015) recommended that minimising on-site erosion rates was ultimately the most effective way to decrease sediment input from arable land to water courses in Switzerland. Our results support this management proposition. However, our simulations also indicate that the disproportional sediment connectivity afforded by the dense road network translates into an excessive sediment supply to water courses, even when simulated erosion rates were small. As on-site erosion rates in Switzerland are already reasonably low (see Prasuhn, 2020), it might be important to consider solutions that address the sediment transport through the underground drainage system, particularly in environmentally sensitive areas, such as the Baldegg catchment.

In a wider context, our study has demonstrated how structural sediment connectivity patterns can be investigated with a conceptual model such as WaTEM/SEDEM, provided that model spatial resolution is sufficiently fine to represent relevant features and processes. In agricultural catchments of the Swiss Plateau and likely in other patchy landscapes, soil redistribution rates and patterns are intrinsically linked to linear features (see Alder et al., 2015; Ledermann et al., 2010; Prasuhn, 2020; Remund et al., 2021). Hence, in order to provide relevant system descriptions, soil erosion models applied under similar conditions must be able to represent linear features and landscape patchiness. Although our results might seem case-specific, similar findings have been reported around the world. For instance, the effects of roads and farm tracks in both coupling and decoupling runoff and sediments has been described in Australia (Croke et al., 2005), Brazil (Bispo et al., 2020), Kenya (Stenfert Kroese et al., 2020), Italy (Persichillo et al., 2018), Spain (Calsamiglia et al., 2018), and the USA (Mahoney et al., 2018). Moreover, the influence of linear features such as field borders, hedges, terraces, and tractor tram lines on soil redistribution rates have been well documented in Europe (Calsamiglia et al., 2018b; Evrard et al., 2009; Fiener and Auerswald, 2005; Lacoste et al., 2014; Saggau et al., 2019), as well as the importance of landscape structure in regulating sediment connectivity (Baartman et al., 2020; Chartin et al., 2013; Fiener et al., 2011).

Another generalisable finding from our research was that WaTEM/SEDEM can be as sensitive to RUSLE parameters as to the model-specific transport capacity coefficients. Therefore, when performing uncertainty analyses of WaTEM/SEDEM, it is important to consider sources of error associated to the RUSLE parameterisation. So far, uncertainty estimation methods applied to WaTEM/SEDEM have focused on the K_{TC} parameterisation, and therefore have underestimated the uncertainty in model predictions. We anticipate that our open-source WaTEM/SEDEM script will facilitate stochastic implementations of the model, and ultimately promote uncertainty and sensitivity analysis of soil erosion models. In particular, the open-source code will allow model users to explore structural uncertainties, which can contribute to increase our understanding of sediment connectivity processes. As recent studies

have again demonstrated, investigating the uncertainty in model structures, parameter estimation, and observational testing data is crucial for advancing soil erosion modelling research (Benaud et al., 2021; Eekhout et al., 2021; Schürz et al., 2020).

Importantly, while we demonstrated how conceptual models such as WaTEM/SEDEM can be useful for understanding structural connectivity patterns, more dynamic and process-oriented models are necessary for identifying so-called hot spots and hot moments of sediment connectivity (Owens, 2020; Turnbull and Wainwright, 2019). In addition, WaTEM/SEDEM representations of sediment transfer could be improved by incorporating the (dis)connectivity caused by linear features other than parcel borders and grass buffer strips. This might entail assimilating the P_{Con} parameter to features such as roadside ditches or terraces. Finally, mapping the location of hydraulic shortcuts within the road network, as well as the extent to which these shortcuts increase the connectivity from hillslopes to water courses (e.g., Schönenberger and Stamm, 2021), should further improve sediment connectivity simulations in areas such as the Baldegg catchment.

5 Conclusions

Here we employed a global sensitivity analysis of the WaTEM/SEDEM model to investigate the influence of linear structures and landscape patchiness on sediment connectivity in the Baldegg catchment. In particular, this novel application of WaTEM/SEDEM was implemented with the free programming language R, and our code is available as supplementary material.

Our results demonstrated that assumptions about road connectivity were by far the most important factor for modelling sediment transfer in the Baldegg catchment. Moreover, the comparison between extensive model simulations and sediment rating curve calculations indicated that roads and hydraulic shortcuts are likely to behave as conduits for sediment transport in the catchment. Hence, representing road connectivity is crucial for modelling sediment transfer from hillslope to water courses in this agricultural catchment of the Swiss Plateau, and potentially in other areas with a dense road drainage system. Moreover, our results further highlighted the effects of linear structures and landscape patchiness on sediment connectivity. These findings were made possible by the use of a model that was specifically tailored to explore the particularities of our study area, by effectively exploring model assumptions and the parameter space, and by the use of ~~high resolution~~high-resolution spatial data.

Overall, we found that WaTEM/SEDEM was useful for investigating sediment connectivity in the Baldegg catchment, as it allowed us to unravel some of the processes and structures regulating hillslope sediment transport in the area. In the case the model is used for prediction and decision-making, we recommend employing a fit-for-purpose rejectionist model testing framework, with multiple sources of data, in order to evaluate the model's numerical accuracy and the quality of its spatial predictions.

6 Code availability

~~The code for the model simulations was uploaded as a supplementary material file. If the manuscript is accepted, we will upload the R script file and input data used for the simulations to the EnviDat platform (https://www.envidat.ch).~~The code for the model simulations, sediment rating curves, and random forest analysis is available at https://doi.org/10.5281/zenodo.6560226.

7 Data availability

~~If the manuscript is accepted, we will upload the input data used for the simulations, and the raw sediment and discharge data to the EnviDat platform (https://www.envidat.ch).~~The input data for the model simulations, the raw sediment concentration and discharge data, and model results are available at https://doi.org/10.5281/zenodo.6560226.

8 Author contributions

PVGB and PF developed the model code, PVGB performed the simulations and analysed the data. SS prepared model input data. PVGB prepared the manuscript with contributions from all authors. CA was part of discussing ideas and revised the manuscript.

9 Competing interests

The authors declare no conflict of interest.

10 Acknowledgements

The authors would like to thank Robert Lovas, from the department of environment and energy of the Canton of Lucerne, for supplying the sediment concentration and water discharge monitoring data, and commenting on an earlier draft of this manuscript. We also appreciate the help from Axel Birkholz in acquiring the data. PVGB would like to thank Franz Conen and Claudia Mignani for their multiple and valuable inputs regarding the conceptualisation and preparation of this manuscript. We are thankful to the comments from two anonymous reviewers, which greatly improved the quality of this manuscript.

References

Alder, S., Prasuhn, V., Liniger, H., Herweg, K., Hurni, H., Candinas, A. and Gujer, H. U.: A high-resolution map of direct and indirect connectivity of erosion risk areas to surface waters in Switzerland-A risk assessment tool for planning and policy-making, Land use policy, 48, 236–249, doi:10.1016/j.landusepol.2015.06.001, 2015.

Antoniadis, A., Lambert-Lacroix, S. and Poggi, J. M.: Random forests for global sensitivity analysis: A selective review, Reliab. Eng. Syst. Saf., 206, 107312, doi:10.1016/j.ress.2020.107312, 2021.

von Arb, C., Stoll, S., Frossard, E., Stamm, C. and Prasuhn, V.: The time it takes to reduce soil legacy phosphorus to a tolerable level for surface waters: What we learn from a case study in the catchment of Lake Baldegg, Switzerland, Geoderma, 403, doi:10.1016/j.geoderma.2021.115257, 2021.

Baartman, J. E. M., Nunes, J. P., Masselink, R., Darboux, F., Bielders, C., Degré, A., Cantreul, V., Cerdan, O., Grangeon, T., Fiener, P., Wilken, F., Schindewolf, M. and Wainwright, J.: What do models tell us about water and sediment connectivity?, Geomorphology, 367, 107300, doi:10.1016/j.geomorph.2020.107300, 2020.

BAFU: Faktenblatt: Der Greifensee, Zustand bezüglich Wasserqualität, 1–8 [online] Available from: http://www.bafu.admin.ch, 2016.

Bakker, M. M., Govers, G., van Doorn, A., Quetier, F., Chouvardas, D. and Rounsevell, M.: The response of soil erosion and sediment export to land-use change in four areas of Europe: The importance of landscape pattern, Geomorphology, 98(3–4), 213–226, doi:10.1016/j.geomorph.2006.12.027, 2008.

Batista, P. V. G., Laceby, J. P., Davies, J., Carvalho, T. S., Tassinari, D., Silva, M. L. N., Curi, N. and Quinton, J. N.: A framework for testing large-scale distributed soil erosion and sediment delivery models : Dealing with uncertainty in models and the observational data, Environ. Model. Softw., 137, doi:10.1016/j.envsoft.2021.104961, 2021.

Bauer, M., Dostal, T., Krasa, J., Jachymova, B., David, V., Devaty, J., Strouhal, L. and Rosendorf, P.: Risk to residents, infrastructure, and water bodies from flash floods and sediment transport, Environ. Monit. Assess., 191(2), doi:10.1007/s10661-019-7216-7, 2019.

Benaud, P., Anderson, K., Evans, M., Farrow, L., Glendell, M., James, M. R., Quine, T. A., Quinton, J. N., Rickson, R. J. and Brazier, R. E.: Reproducibility, open science and progression in soil erosion research. A reply to “Response to ‘National-scale geodata describe widespread accelerated soil erosion’ Benaud et al. (2020) Geoderma 271, 114378” by Evans and Boardman (2021), Geoderma, 402, doi:10.1016/j.geoderma.2021.115181, 2021.

Bircher, P., Liniger, H. and Prasuhn, V.: Aktualisierung und Optimierung der Erosionsrisikokarte (ERK2) Die neue ERK2 (2019) für das Ackerland der Schweiz, 2019.

Bispo, D. F. A., Batista, P.V.G., Guimarães, D. V., Silva, M. L. N., Curi, N. and Quinton, J. N.: Monitoring land use impacts on sediment production : a case study of the pilot catchment from the Brazilian program of payment for environmental services, Rev. Bras. Ciência do Solo, 44, :e0190167, 2020.

Boardman, J.: A 38-year record of muddy flooding at Breaky Bottom: Learning from a detailed case study, Catena, 189(January), 104493, doi:10.1016/j.catena.2020.104493, 2020.

Borselli, L., Cassi, P. and Torri, D.: Prolegomena to sediment and flow connectivity in the landscape: A GIS and field numerical assessment, Catena, 75(3), 268–277, doi:10.1016/j.catena.2008.07.006, 2008.

Breiman, L.: Random forests, Machine Learning, 45, 5-32, 2001.

Brenning, A., Bangs, D., Becker, M.: RSAGA: SAGA geoprocessing and terrain analysis. R package version 1.3.0., 2018.

Calsamiglia, A., García-Comendador, J., Fortesa, J., López-Tarazón, J. A., Crema, S., Cavalli, M., Calvo-Cases, A. and Estrany, J.: Effects of agricultural drainage systems on sediment connectivity in a small Mediterranean lowland catchment, Geomorphology, 318, 162–171, doi:10.1016/j.geomorph.2018.06.011, 2018a.

Calsamiglia, A., Fortesa, J., García-Comendador, J., Lucas-Borja, M. E., Calvo-Cases, A. and Estrany, J.: Spatial patterns of sediment connectivity in terraced lands: Anthropogenic controls of catchment sensitivity, L. Degrad. Dev., 29(4), 1198–1210, doi:10.1002/ldr.2840, 2018b.

Cavalli, M., Trevisani, S., Comiti, F. and Marchi, L.: Geomorphometric assessment of spatial sediment connectivity in small Alpine catchments, Geomorphology, 188, 31–41, doi:10.1016/j.geomorph.2012.05.007, 2013.

Chartin, C., Evrard, O., Salvador-Blanes, S., Hinschberger, F., Van Oost, K., Lefèvre, I., Daroussin, J. and Macaire, J. J.: Quantifying and modelling the impact of land consolidation and field borders on soil redistribution in agricultural landscapes (1954-2009), Catena, 110, 184–195, doi:10.1016/j.catena.2013.06.006, 2013.

Cohn, T. A., Caulder, D. L., Gilroy, J., Zynjuk, L. D. and Summers, R. M.: The Validity of a Simple Statistical Model for Estimating, Water Resour. Res., 28(9), 2353–2363, 1992.

Conrad, O., Bechtel, B., Bock, M., Dietrich, H., Fischer, E., Gerlitz, L., Wehberg, J., Wichmann, V. and Böhner, J.: System for Automated Geoscientific Analyses (SAGA) v.2.2.2, 1991–2007, doi:10.5194/gmd-8-1991-2015, 2015.

651 Croke, J., Mockler, S., Fogarty, P. and Takken, I.: Sediment concentration changes in runoff pathways
652 from a forest road network and the resultant spatial pattern of catchment connectivity,
653 Geomorphology, 68(3–4), 257–268, doi:10.1016/j.geomorph.2004.11.020, 2005.

654 Desmet, P., Govers, G.: A GIS procedure for automatically calculating the USLE LS factor on
655 topographically complex landscape units, J. Soil Water Conserv., 51, 427–433, 1996.

656 Eekhout, J. P. C., Millares-Valenzuela, A., Martínez-Salvador, A., García-Lorenzo, R., Pérez-Cutillas,
657 P., Conesa-García, C. and de Vente, J.: A process-based soil erosion model ensemble to assess model
658 uncertainty in climate-change impact assessments, L. Degrad. Dev., 32, 2409–2422,
659 doi:10.1002/ldr.3920, 2021.

660 Evrard, O., Cerdan, O., van Wesemael, B., Chauvet, M., Le Bissonnais, Y., Raclot, D., Vandaele, K.,
661 Andrieux, P. and Bielders, C.: Reliability of an expert-based runoff and erosion model: Application of
662 STREAM to different environments, Catena, 78(2), 129–141, doi:10.1016/j.catena.2009.03.009, 2009.

663 Fiener, P. and Auerswald, K.: Measurement and modeling of concentrated runoff in grassed
664 waterways, J. Hydrol., 301(1–4), 198–215, doi:10.1016/j.jhydrol.2004.06.030, 2005.

665 Fiener, P., Auerswald, K. and Van Oost, K.: Spatio-temporal patterns in land use and management
666 affecting surface runoff response of agricultural catchments-A review, Earth-Science Rev., 106(1–2),
667 92–104, doi:10.1016/j.earscirev.2011.01.004, 2011.

668 Fiener, P., Wilken, F. and Auerswald, K.: Filling the gap between plot and landscape scale – eight
669 years of soil erosion monitoring in 14 adjacent watersheds under soil conservation at Scheyern,
670 Southern Germany, Adv. Geosci. Discuss., (July), doi:adgeo-2019-4, 2019.

671 Fryirs, K.: (Dis)Connectivity in catchment sediment cascades: A fresh look at the sediment delivery
672 problem, Earth Surf. Process. Landforms, 38(1), 30–46, doi:10.1002/esp.3242, 2013.

673 Gelman, A. and Hill, J.: Data Analysis Using Regression and Multilevel/Hierarchical Models,
674 Cambridge Univeristy Press, New York., R package version 1.12.2, 2007.

675 Govers, G.: Misapplications and misconceptions of erosion models, in: Handbook of erosion
676 modelling, edited by: Morgan, R. P. C., Nearing, M.A., Blackwell Publishing Ltd., Chichester, United
677 Kingdom, 117–134, 2011.

678 Heckmann, T., Cavalli, M., Cerdan, O., Foerster, S., Javaux, M., Lode, E., Smetanová, A., Vericat, D.
679 and Brardinoni, F.: Indices of sediment connectivity: opportunities, challenges and limitations, Earth-
680 Science Rev., 187(December 2017), 77–108, doi:10.1016/j.earscirev.2018.08.004, 2018.

681 IUSS Working Group WRB. World Reference Base for Soil Resources; IUSS Working Group WRB:
682 Wageningen, The Netherlands, 2006; pp. 1–128.

683 Keller, B.: Lake Lucerne and its spectacular landscape, in: Landscapes and landforms of Switzerland,
684 edited by Reynard, E., Springer Nature Switzerland, Cham, Switzerland, 305-324, 2021.

685 Krasa, J., Dostal, T., Jachymova, B., Bauer, M. and Devaty, J.: Soil erosion as a source of sediment
686 and phosphorus in rivers and reservoirs – Watershed analyses using WaTEM/SEDEM, Environ. Res.,
687 171(January), 470–483, doi:10.1016/j.envres.2019.01.044, 2019.

688 Kupferschmied, P.: CP-Tool: Ein Programm zur Berechnung des Fruchtfolge- und
689 Bewirtschaftungsfaktors (CP-Faktor) der Allgemeinen Bodenabtragsgleichung (ABAG), 2019.

690 Laceby, J. P., Batista, P. V. G., Taube, N., Kruk, M. K., Chung, C., Evrard, O. and Orwin, J. F.:
691 Tracing total and dissolved material in a western Canadian basin using quality control samples to
692 guide the selection of fingerprinting parameters for modelling, Catena, 200(April 2020), 105095,
693 doi:10.1016/j.catena.2020.105095, 2021.

694 Lacoste, M., Michot, D., Viaud, V., Evrard, O. and Walter, C.: Combining137Cs measurements and a
695 spatially distributed erosion model to assess soil redistribution in a hedgerow landscape in
696 northwestern France (1960-2010), Catena, 119, 78–89, doi:10.1016/j.catena.2014.03.004, 2014.

697 Lavrieux, M., Birkholz, A., Meusburger, K., Wiesenberg, G. L. B., Gilli, A., Stamm, C. and Alewell,
698 C.: Plants or bacteria? 130 years of mixed imprints in Lake Baldegg sediments (Switzerland), as
699 revealed by compound-specific isotope analysis (CSIA) and biomarker analysis, Biogeosciences,
700 16(10), 2131–2146, doi:10.5194/bg-16-2131-2019, 2019.

701 Ledermann, T., Herweg, K., Liniger, H. P., Schneider, F., Hurni, H. and Prasuhn, V.: Applying
702 erosion damage mapping to assess and quantify off-site effects of soil erosion in Switzerland, L.
703 Degrad. Dev., 21, 353–366, 2010.

704 Liaw, A., Wiener, M.: Classification and regression by randomForest. R News, 2, 18–22, R package
705 version 4.7.1, 2002.

706 Mahoney, D. T., Fox, J. F. and Al-Aamery, N.: Watershed erosion modeling using the probability of
707 sediment connectivity in a gently rolling system, J. Hydrol., 561(April), 862–883,
708 doi:10.1016/j.jhydrol.2018.04.034, 2018.

709 Mahoney, D. T., Fox, J., Al-Aamery, N. and Clare, E.: Integrating connectivity theory within
710 watershed modelling part I: Model formulation and investigating the timing of sediment connectivity,
711 Sci. Total Environ., 740, 140385, doi:10.1016/j.scitotenv.2020.140385, 2020a.

712 Mahoney, D. T., Fox, J., Al-Aamery, N. and Clare, E.: Integrating connectivity theory within
713 watershed modelling part II: Application and evaluating structural and functional connectivity, Sci.
714 Total Environ., 740, 140386, doi:10.1016/j.scitotenv.2020.140386, 2020b.

715 MeteoSwiss. SwissMetNet Surface Weather Stations, Mosen MOA, 2010-2019 (Switzerland), 2021.

Müller, B., Gächter, R. and Wüest, A.: Accelerated water quality improvement during oligotrophication in peri-alpine lakes, Environ. Sci. Technol., 48(12), 6671–6677, doi:10.1021/es4040304, 2014.

Notebaert, B., Vaes, B., Govers, G., Van Oost, K., Van Rompaey, A., and Verstraeten, G.: WaTEM / SEDEM version 2006 Manual., 2006.

Nunes, J. P., Wainwright, J., Bielders, C. L., Darboux, F., Fiener, P., Finger, D. and Turnbull, L.: Better models are more effectively connected models, Earth Surf. Process. Landforms, 43(6), 1355–1360, doi:10.1002/esp.4323, 2018.

Owens, P. N.: Soil erosion and sediment dynamics in the Anthropocene: a review of human impacts during a period of rapid global environmental change, J. Soils Sediments, 20(12), 4115–4143, doi:10.1007/s11368-020-02815-9, 2020.

Parsons, A. J., Wainwright, J., Brazier, R. E. and Powell, D. M.: Is sediment delivery a fallacy? Reply, Earth Surf. Process. Landforms, 34(February), 155–161, doi:10.1002/esp, 2009.

Persichillo, M. G., Bordoni, M., Cavalli, M., Crema, S. and Meisina, C.: The role of human activities on sediment connectivity of shallow landslides, Catena, 160(August 2016), 261–274, doi:10.1016/j.catena.2017.09.025, 2018.

Pianosi, F., Beven, K., Freer, J., Hall, J. W., Rougier, J., Stephenson, D. B. and Wagener, T.: Sensitivity analysis of environmental models: A systematic review with practical workflow, Environ. Model. Softw., 79, 214–232, doi:10.1016/j.envsoft.2016.02.008, 2016.

Pfiffner, O. A.: The structural landscapes of Central Switzerland, in: Landscapes and landforms of Switzerland, edited by Reynard, E., Springer Nature Switzerland, Cham, Switzerland, 159-172, 2021.

Prasuhn, V.: Twenty years of soil erosion on-farm measurement: annual variation, spatial distribution and the impact of conservation programmes for soil loss rates in Switzerland, Earth Surf. Process. Landforms, doi:10.1002/esp.4829, 2020.

Remund, D., Liebisch, F., Liniger, H. P., Heinimann, A. and Prasuhn, V.: The origin of sediment and particulate phosphorus inputs into water bodies in the Swiss Midlands – A twenty-year field study of soil erosion, Catena, 203(March), 105290, doi:10.1016/j.catena.2021.105290, 2021.

Renard, K., Foster, G. R., Weesies, G. A., McCool, D. K. and Yoder, D. C.: Predicting Soil Erosion by Water: A Guide to Conservation Planning With the Revised Universal Soil Loss Equation (RUSLE), 1997.

R Core Team. R: A language for statistical computing. R Foundation for Statistical Computing, Vienna, Austria. URL https://www.R-project.org, 2021.

748 Saggau, P., Kuhwald, M. and Duttmann, R.: Integrating soil compaction impacts of tramlines into soil
749 erosion modelling: A field-scale approach, Soil Syst., 3(3), 1–28, doi:10.3390/soilsystems3030051,
750 2019.

751 Schmidt, S., Alewell, C., Panagos, P. and Meusburger, K.: Regionalization of monthly rainfall
752 erosivity patternsin Switzerland, Hydrol. Earth Syst. Sci., 20(10), 4359–4373, doi:10.5194/hess-20-
753 4359-2016, 2016.

754 Schmidt, S., Ballabio, C., Alewell, C., Panagos, P. and Meusburger, K.: Filling the European blank
755 spot—Swiss soil erodibility assessment with topsoil samples, J. Plant Nutr. Soil Sci., 181(5), 737–748,
756 doi:10.1002/jpln.201800128, 2018a.

757 Schmidt, S., Alewell, C. and Meusburger, K.: Mapping spatio-temporal dynamics of the cover and
758 management factor (C-factor) for grasslands in Switzerland, Remote Sens. Environ., 211(April), 89–
759 104, doi:10.1016/j.rse.2018.04.008, 2018b.

760 Schönenberger, U. and Stamm, C.: Hydraulic shortcuts increase the connectivity of arable land areas
761 to surface waters, Hydrol. Earth Syst. Sci., 25(4), 1727–1746, doi:10.5194/hess-25-1727-2021, 2021.

762 Schürz, C., Mehdi, B., Kiesel, J., Schulz, K. and Herrnegger, M.: A systematic assessment of
763 uncertainties in large-scale soil loss estimation from different representations of USLE input factors-a
764 case study for Kenya and Uganda, Hydrol. Earth Syst. Sci., 24(9), 4463–4489, doi:10.5194/hess-24-
765 4463-2020, 2020.

766 Sherriff, S. C., Rowan, J. S., Fenton, O., Jordan, P., Melland, A. R., Mellander, P. E. and Huallacháin,
767 D.: Storm Event Suspended Sediment-Discharge Hysteresis and Controls in Agricultural Watersheds:
768 Implications for Watershed Scale Sediment Management, Environ. Sci. Technol., 50(4), 1769–1778,
769 doi:10.1021/acs.est.5b04573, 2016.

770 Starkloff, T. and Stolte, J.: Applied comparison of the erosion risk models EROSION 3D and LISEM
771 for a small catchment in Norway, Catena, 118, 154–167, doi:10.1016/j.catena.2014.02.004, 2014.

772 Stenfert Kroese, J., Batista, P. V. G., Jacobs, S. R., Breuer, L., Quinton, J. N. and Rufino, M. C.:
773 Agricultural land is the main source of stream sediments after conversion of an African montane
774 forest, Sci. Rep., 10(1), 1–15, doi:10.1038/s41598-020-71924-9, 2020.

775 Stoll, S., Arb, C. von, Jorg, C., Kopp, S. and Prasuhn, V.: Evaluation der stark zur Phosphor-Belastung
776 des Baldeggersees beitragenden Flächen., 2019.

777 Swisstopo. SwissALTI3D. Das hoch aufgelöste Terrainmodell der Schweiz, 2014a.

778 Swisstopo. Swissimage. Das digitale Farborthophotomosaik der Schweiz. 2014b.

779 Swisstopo. Swiss Map Vector 25 Beta, Das digitale Landschaftsmodell der Schweiz. 2018.

Swisstopo. SwissTLM3D. Das grossmassstäbliche Topografische Landschaftsmodell der Schweiz, 2020.

Teranes, J. L. and Bernasconi, S. M.: Factors controlling δ13C values of sedimentary carbon in hypertrophic Baldeggersee, Switzerland, and implications for interpreting isotope excursions in lake sedimentary records, Limnol. Oceanogr., 50(3), 914–922, doi:10.4319/lo.2005.50.3.0914, 2005.

Turnbull, L. and Wainwright, J.: From structure to function: Understanding shrub encroachment in drylands using hydrological and sediment connectivity, Ecol. Indic., 98(November 2018), 608–618, doi:10.1016/j.ecolind.2018.11.039, 2019.

Van Oost, K., Govers, G. and Desmet, P. J. J.: Evaluating the effects of changes in landscape structure on soil erosion by water and tillage, Landsc. Ecol., 15(6), 577–589, doi:10.1023/A:1008198215674, 2000.

Van Rompaey, A., Verstraeten, G., Van Oost, K., Govers, G. and Poesen, J.: Modelling mean annual sediment yield using a distributed approach, Earth Surf. Process. Landforms, 26(11), 1221–1236, doi:10.1002/esp.275, 2001.

Verstraeten, G., Van Oost, K., Van Rompaey, A. J. J., Poesen, J. and Govers, G.: Evaluating an integrated approach to catchment management to reduce soil loss and sediment pollution through modelling, Soil Use Manag., 18(4), 386–394, doi:10.1111/j.1475-2743.2002.tb00257.x, 2010.

Vigiak, O. and Bende-Michl, U.: Estimating bootstrap and Bayesian prediction intervals for constituent load rating curves, Water Resour. Res., 49(12), 8565–8578, doi:10.1002/2013WR013559, 2013.

Wainwright, J., Turnbull, L., Ibrahim, T. G., Lexartza-Artza, I., Thornton, S. F. and Brazier, R. E.: Linking environmental regimes, space and time: Interpretations of structural and functional connectivity, Geomorphology, 126(3–4), 387–404, doi:10.1016/j.geomorph.2010.07.027, 2011.

~~Wang, Y. G., Kuhnert, P. and Henderson, B.: Load estimation with uncertainties from opportunistic sampling data - A semiparametric approach, J. Hydrol., 396(1–2), 148–157, doi:10.1016/j.jhydrol.2010.11.003, 2011.~~

Wehrli, B., Lotter, A. F., Schaller, T. and Sturm, M.: High-resolution varve studies in Baldeggersee (Switzerland): Project overview and limnological background data, Aquat. Sci., 59(4), 285–294, doi:10.1007/BF02522359, 1997.

Wilken, F., Fiener, P. and Van Oost, K.: Modelling a century of soil redistribution processes and carbon delivery from small watersheds using a multi-class sediment transport model, Earth Surf. Dyn., 5, 113–124, doi:10.5194/esurf-5-113-2017, 2017.